Genes & Diseases (2018) 5, 137–149

Available online at www.sciencedirect.com

ScienceDirect

journal homepage: http://ees.elsevier.com/gendis/default.asp

FULL LENGTH ARTICLE

Establishment and functional characterization of the reversibly immortalized mouse glomerular podocytes (imPODs)

Xinyi Yu [a,b], Liqun Chen [a,b], Ke Wu [b,c], Shujuan Yan [b,c], Ruyi Zhang [b,c], Chen Zhao [a,b], Zongyue Zeng [b,c], Yi Shu [b,c], Shifeng Huang [a,b], Jiayan Lei [a,b], Xiaojuan Ji [a,b], Chengfu Yuan [b,d], Linghuan Zhang [b,c], Yixiao Feng [a,b], Wei Liu [a,b], Bo Huang [b,c,e], Bo Zhang [b,f], Wenping Luo [b,c], Xi Wang [b,c], Bo Liu [a,b], Rex C. Haydon [b], Hue H. Luu [b], Tong-Chuan He [b], Hua Gan [a,*]

[a] *Departments of Nephrology, Orthopaedic Surgery, Cardiology, General Surgery, Plastic Surgery, and Clinical Laboratory Medicine, The First Affiliated Hospital of Chongqing Medical University, Chongqing, 400016, China*
[b] *Molecular Oncology Laboratory, Department of Orthopaedic Surgery and Rehabilitation Medicine, The University of Chicago Medical Center, Chicago, IL, 60637, USA*
[c] *Ministry of Education Key Laboratory of Diagnostic Medicine and School of Laboratory Medicine, and the Affiliated Hospitals of Chongqing Medical University, Chongqing, 400016, China*
[d] *Department of Biochemistry and Molecular Biology, China Three Gorges University School of Medicine, Yichang, 443002, China*
[e] *Department of Clinical Laboratory Medicine, The Second Affiliated Hospital of Nanchang University, Nanchang, 330031, China*
[f] *Key Laboratory of Orthopaedic Surgery of Gansu Province and the Department of Orthopaedic Surgery, The Second Hospital of Lanzhou University, Lanzhou, 730030, China*

Received 10 April 2018; accepted 17 April 2018
Available online 23 April 2018

* Corresponding author. Department of Nephrology, The First Affiliated Hospital, Chongqing Medical University, Chongqing, 400016, China.
E-mail address: ghzxgckd@163.com (H. Gan).
Peer review under responsibility of Chongqing Medical University.

https://doi.org/10.1016/j.gendis.2018.04.003

KEYWORDS
Chronic kidney disease;
FLP recombinase;
Glomerular disease;
Glomerulus;
Immortalization;
Nephropathy;
Podocyte;
SV40 T antigen

Abstract Glomerular podocytes are highly specialized epithelial cells and play an essential role in establishing the selective permeability of the glomerular filtration barrier of kidney. Maintaining the viability and structural integrity of podocytes is critical to the clinical management of glomerular diseases, which requires a thorough understanding of podocyte cell biology. As mature podocytes lose proliferative capacity, a conditionally SV40 mutant tsA58-immortalized mouse podocyte line (designated as tsPC) was established from the Immortomouse over 20 years ago. However, the utility of the tsPC cells is hampered by the practical inconvenience of culturing these cells. In this study, we establish a user-friendly and reversibly-immortalized mouse podocyte line (designated as imPOD), on the basis of the tsPC cells by stably expressing the wildtype SV40 T-antigen, which is flanked with FRT sites. We show the imPOD cells exhibit long-term high proliferative activity, which can be effectively reversed by FLP recombinase. The imPOD cells express most podocyte-related markers, including WT-1, Nephrin, Tubulin and Vinculin, but not differentiation marker Synaptopodin. The imPOD cells do not form tumor-like masses *in vivo*. We further demonstrate that TGFβ1 induces a podocyte injury-like response in the FLP-reverted imPOD cells by suppressing the expression of slit diaphragm-associated proteins P-Cadherin and ZO-1 and upregulating the expression of mesenchymal markers, α-SMA, Vimentin and Nestin, as well as fibrogenic factors CTGF and Col1a1. Collectively, our results strongly demonstrate that the newly engineered imPOD cells should be a valuable tool to study podocyte biology both under normal and under pathological conditions.

Introduction

Glomerular podocytes in kidney are highly specialized visceral epithelial cells and have a complex cytoarchitecture of interdigitated foot processes with filtration slits in between.[1–3] Such slit diaphragm system plays an essential role in establishing the selective permeability of the glomerular filtration barrier. Podocytes are involved in a variety of glomerular functions, including glomerular basement membrane (GBM) turnover, maintenance of filtration barrier, support of the capillary tuft, regulation of glomerular filtration and immunological functions.[1,2,4] According to the cellular architecture, podocytes can be divided into three structurally and functionally different segments: cell body, major process and foot process.[1,2,4] There are many major processes attaching to the cell body, as well as primary, then secondary, and some tertiary MPs branching from the cell body.[1,2,4] During podocyte differentiation, numerous primary and secondary foot processes are extended from the cell, usually emerging at right angles to the major processes and contacting with the GBM.[1,2,4] The GBM and the filtration slits between the podocytes perform the filtration function of the glomerulus.

The glomerular podocytes play an important role in the physiology and pathophysiology of the glomerulus.[1,2,4] Injury to podocytes may lead to proteinuria, a hallmark of most glomerular diseases and chronic kidney disease, and disruptions of podocyte architecture resulting in the retraction of foot processes and proteinuria are common features in the progression of acquired glomerular disease.[3,5] Thus, maintaining podocyte viability and structural integrity is critical to the clinical management of glomerular diseases and chronic kidney disease, which requires a thorough understanding of podocyte cell biology.

Once in the mature state, podocytes lose the proliferative capacity and form specialized junctions between the cell body and the GBM, known as the focal adhesion complex, and junctions between interdigitating foot processes, known as the slit diaphragm or membrane.[1,2,4,6] For a long time, the selective analysis of podocytes *in vitro* was difficult as only rather undifferentiated "podocytes" of questionable cellular origin were available in culture.[6,7] Moreover, culturing podocytes under standard conditions leads to dedifferentiation and the loss of processes.[7] A breakthrough came when a mouse podocyte line was derived from immortomouse in 1996.[7] The established mouse podocytes are conditionally immortalized by using the temperature-sensitive (*ts*) mutant form of SV40 mutant tsA58 driven by a γ-interferon (γ-INF)-responsive promoter.[7] Thus, such SV40 mutant tsA58 conditionally immortalized mouse podocytes (designated as tsPC in the text thereafter) can be cultured in two conditions yielding different phenotypes. Under permissive conditions (i.e., at 33 °C with γ-INF, or tsPC-33 °C), these cells proliferate and adapt an epithelial phenotype with cobblestone-like morphology. On the contrary, the tsPC cells stop proliferating and differentiate into arborized cells under nonpermissive conditions (i.e., at 37 °C without γ-INF, or tsPC-37 °C). The tsPC cells have offered unique opportunities for studying the physiology and pathophysiology of podocytes for the past 20 years. Nonetheless, the practical utility of the tsPC cells has been limited by the fact that it is time-consuming, laborious, and inconvenient to maintain the tsPC line, which requires culturing at 33 °C and γ-IFN to induce the expression of functional SV40 T antigen.

Here, in order to overcome the practical inconvenience of culturing and using the tsPC cells, we establish the reversibly immortalized mouse podocytes (designated as imPOD) on the basis of the parental tsPC cells. The newly established imPOD cells are immortalized by stably expressing the wildtype SV40 T-antigen, which is flanked with the Flippase Recognition Target (FRT) sites as described in our previous studies.[8–21] We demonstrate that the imPOD cells exhibit long-term high proliferative activity, which can be effectively reversed by Flippase (FLP) recombinase. The imPOD cells express most of the podocyte-related markers, do not form tumors *in vivo* and exhibit the characteristics similar to mature podocytes upon TGFβ1 stimulation. Thus, the imPOD cells are stable, reversible and non-tumorigenic podocyte-like cells, which should be a valuable resource to study podocyte biology both under normal and under pathological conditions.

Materials and methods

Cell culture and chemicals

HEK-293 and human renal cancer line Caki-1 were obtained from ATCC (Manassas, VA). 293pTP and RAPA cells were previously characterized.[22,23] All of these cell lines were maintained in the completed Dulbecco's modified Eagle medium (DMEM) as described.[13,24–26] The parental SV40 T-antigen temperature sensitive-mutant immortalized mouse podocytes (designated as tsPC cells) were kindly provided by Dr. Yan-Chun Li of The University of Chicago and maintained under permissive conditions at 33 °C with RPMI 1640 containing 10% FBS, 100 U/ml γ-IFN, and 100 U/ml penicillin/streptomycin as described.[7,27] Unless indicated otherwise, all chemicals were purchased from Sigma–Aldrich (St. Louis, MO, USA) or Thermo Fisher Scientific (Waltham, MA, USA).

Establishment of reversibly immortalized mouse podocytes (imPOD)

The use of the retroviral vector SSR #41 to express SV40 T antigen flanked with the FRT sites were previously described.[8–21] Briefly, the SSR #41 vector and pCL-Ampho packaging vector were co-transfected into HEK-293 cells to produce the packaged retrovirus. Exponentially growing parental mouse tsPC cells (maintained under permissive conditions at 33 °C with 100 U/ml γ-IFN)[7,27] were infected with the SSR #41 retrovirus and subjected to hygromycin B selection (0.3 mg/ml) for 5–7 days in complete DMEM at 37 °C, yielding the stably immortalized mouse podocytes, designated as the imPOD cell line.

Construction of recombinant adenoviruses expressing TGFβ1, Flippase (FLP), Green Fluorescent Protein (GFP) and monomeric Red Fluorescent Protein (RFP)

Recombinant adenoviruses were generated using the AdEasy technology as previously described.[28–32] Briefly, the coding regions of mouse TGFβ1 and FLP recombinase were PCR amplified and cloned into an adenoviral shuttle vector and subsequently used to generate recombinant adenoviruses in HEK-293, 293pTP or RAPA cells.[22,23] The resulting adenoviruses were designated as Ad-TGFβ1 and Ad-FLP, both of which also express GFP as the marker for monitoring infection efficiency. Analogous adenovirus expressing only GFP or RFP (Ad-GFP or Ad-RFP) was used as a mock control as described.[25,33–37] In order to enhance transgene transduction efficiency, polybrene (8 μg/ml) was added to the culture medium for all adenovirus infections.[38]

Crystal violet assay

Crystal violet assay of cell proliferation was carried out as described.[21,39–44] Briefly, subconfluent imPOD and/or tsPC cells were seeded in 35 mm cell culture dishes and infected with the Ad-FLP or Ad-GFP adenovirus. The cells were subjected to crystal violet staining at the indicated time points. Macrographic staining images were recorded for the stained dishes. For quantitative measurement, the stained cells were dissolved in 10% acetic acid at room temperature with agitation and optical density was measured at 570nm.[45,46]

WST-1 cell proliferation assay

WST-1 assay was carried out as described.[47,48] Briefly, exponentially growing cells were plated into 96-well culture plates at 30% confluence. Unseeded blank wells were utilized as background controls. At the indicated time points, the premixed WST-1 (BD Clontech, Mountain View, CA, USA) was added to each well and incubated at the 37 °C CO_2 incubator for 3 h. The plates were subjected to a microtitre plate reader to obtain absorbance reading at 450 nm. The obtained A450 nm values were subjected to background subtractions. Each assay condition was performed in triplicate.[49,50]

Immunofluorescence staining

Immunofluorescence staining was performed as described.[11,21,51–53] Briefly, subconfluent imPOD or tsPC cells were seeded in 24-well plates overnight, fixed with 4% paraformaldehyde, permeabilized with 1% NP-40, and blocked with 10% donkey serum (Jackson Immuno-Research Laboratories, West Grove, PA, USA), followed by incubating with the WT-1, Synaptopodin, Nephrin, Tubulin or Vinculin mouse monoclonal antibody (Santa Cruz Biotechnology, Dallas, TX, USA) for 2 hrs at room temperature.[11,51,52] After being washed, cells were incubated with FITC labeled anti-mouse IgG secondary antibody (Jackson ImmunoResearch Laboratories, West Grove, PA) for 30 min. The cell nuclei were counterstained with DAPI. Stains without primary antibodies were used as negative controls. Fluorescence images were recorded under an inverted fluorescence microscope.

RNA isolation and Touchdown qPCR (TqPCR) analysis

Subconfluent cells were seeded in 60-mm dishes in a complete DMEM. Total RNA was isolated using TRIzol Reagents (Invitrogen, Carlsbad, CA, USA) as described.[54–56] The cDNA synthesis was carried out using hexamer and M-MuLV

Reverse Transcriptase (New England Biolabs, Ipswich, MA, USA). The cDNA products were diluted 10- to 50-fold and used as PCR templates. The qPCR primers (Supplemental Table 1) were designed using Primer3 Plus.[57] The TqPCR program was carried out as follows[58]: 95 °C × 3 s for one cycle; 95 °C × 20 s, 66 °C × 10 s, for 4 cycles by decreasing 3 °C per cycle; 95 °C × 20 s, 55 °C × 10 s, 70 °C × 1 s, followed by plate read, for 40 cycles using the 2× SYBR Green qPCR master mix (Bimake, Houston, TX).[58] Each assay condition was performed in triplicate. All samples were normalized to Gapdh expression by using the $2^{-\Delta\Delta Ct}$ method as described[54,55]

Subcutaneous cell implantation and Xenogen bioluminescence imaging

The use and care of animals was approved by the Institutional Animal Care and Use Committee. Briefly, the human renal cancer line Caki-1 and imPOD cells were stably labeled with firefly luciferase using our homemade *piggyBac* transposon system,[52,59] yielding Caki-FLuc and imPOD-FLuc, respectively. Exponentially growing Caki-FLuc and imPOD-Fluc cells were collected and injected subcutaneously into the flanks of athymic nude mice (Harlan Laboratories, 6—8 week old, male, 10^6 cells per injection, 4 sites per mouse, n = 5/group). At 1, 7 and 14 days after implantation, the animals were subjected to bioluminescence imaging using Xenogen IVIS 200 imaging system as described.[49,60,61] Briefly, mice were injected (i.p.) with D-Luciferin sodium salt (Gold Biotechnology) at 100 mg/kg in 0.1 ml PBS. The pseudo images were obtained by superimposing the emitted light over the gray-scale photographs of the mice. Quantitative analysis was conducted with Xenogen's Living Image software as described.[49,60,61]

Statistical analysis

All quantitative experiments were performed in triplicate and/or repeated three times. Data were expressed as mean ± standard deviation (SD). The one-way analysis of variance was used to analyze statistical significance.[41] A value of $p < 0.05$ was considered statistically significant.

Results

Establishment of the reversibly immortalized mouse podocytes (imPOD)

Although the conditionally immortalized mouse podocyte line by an SV40 T-antigen ts-mutant (tsPC) was created over 20 years ago,[7] the practical utility of the tsPC cells has been limited by the fact that it is time-consuming, laborious, and inconvenient to maintain the tsPC line, which requires culturing at 33 °C and γ-IFN to induce the expression of functional SV40 T antigen. Here, we sought to establish a reversibly immortalized mouse podocytes based on the parental tsPC cells.

Experimentally, the subconfluent parental tsPC cells were infected with retroviral SSR#41 preparation. The SSR #41 vector contains antibiotic marker hygromycin and SV40 T antigen expression cassette flanked with FRT sites (Fig. 1A).[8] The infected tsPC cells were cultured under nonpermissive conditions at 37 °C with DMEM containing 10% FBS and 100U/ml penicillin/streptomycin. After hygromycin selection, the surviving cells were observed at as early as at 3 days after selection and colonies became more obvious after 3 passages, yielding the imPOD line (Fig. 1B, panel a). The resulting imPOD cells grew rapidly and maintained a high proliferation rate after 20 passages (Fig. 1B, panel a). By now, the imPOD cells have been passed consecutively for over 50 generations and are proliferating well (data not shown). As expected, the parental tsPC cells grew poorly under nonpermissive conditions (at 37 °C without γ-IFN; e.g., tsPC-37 °C) while proliferating well under permissive conditions (at 33 °C with γ-IFN; e.g., tsPC-33 °C) (Fig. 1B, panels *b vs. c*).

Furthermore, we performed qPCR analysis to determine the expression levels of SV40 T antigen in these cell lines. Our results demonstrated that the imPOD cells expressed a higher level of SV40 T antigen than that in the parental tsPC cells cultured under permissive conditions (i.e., tsPC-33 °C) (Fig. 1C), indicating that we have successfully immortalized the mouse podocytes derived from mouse tsPC cells.

The imPOD cells exhibit higher proliferative activity than the parental tsPC cells

We next compared the proliferative activities between the imPOD cells and the parental tsPC cells under both permissive and nonpermissive conditions. Using crystal violet staining assay, we found that when seeded at a similar initial cell density, the imPOD cells reached confluence faster than the parental tsPC-33 °C cells, while both imPOD and tsPC-33 °C cells grew much faster than tsPC-37 °C cells at the tested time points (Fig. 2A, panel a). Quantitative assessment of the stained cells indicated that both imPOD and tsPC-33 °C cells grew much faster than tsPC-37 °C cells from day 2 to day 5, while imPOD cells grew faster than tsPC-33 °C cells at day 4 and day 5 (Fig. 2A, panel b). We obtained similar results by using the more quantitative WST-1 cell proliferation assay (Fig. 2B). Collectively, the above results demonstrate that the imPOD cells can be stably maintained in culture and exhibit a high proliferative rate.

The imPOD cells express most of the podocyte markers

We tested whether the immortalization process would affect the expression of podocyte markers. It has been reported that Wims' tumor gene product WT-1 is exclusively expressed by podocytes in the adult kidney.[62,63] Our immunofluorescence analysis indicated that all imPOD cells, as well as the tsPC-33 °C cells, expressed a high level of nuclear WT-1 protein (Fig. 3A). However, neither groups expressed a detectable level of Synaptopodin (Fig. 3A), which is a differentiation-specific actin cytoskeleton-associated protein and only expressed in differentiating podocytes,[7,64] suggesting the imPOD cells may possess differentiation potential.

We further analyzed whether the genes required for the formation of the slit diaphragm complex (such as Nephrin,

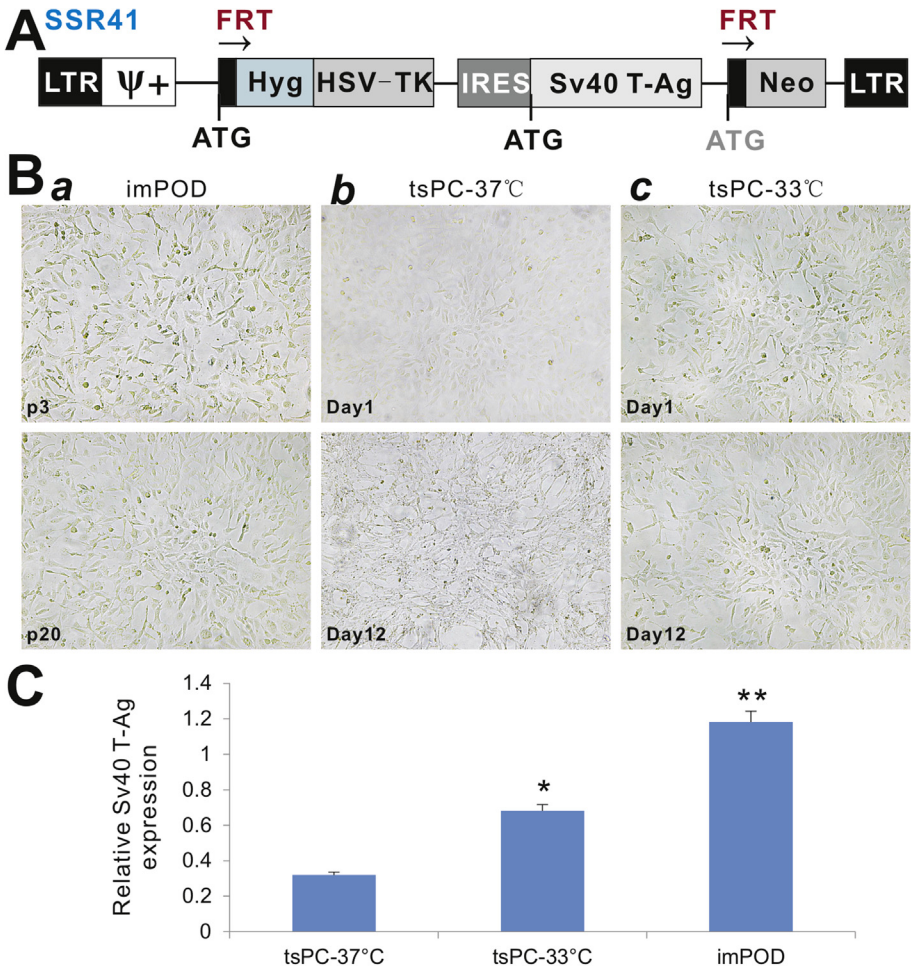

Figure 1 Establishment of the reversibly immortalized mouse podocytes (imPOD) from the parental tsPC cells. (**A**) Schematic representation of the reversible immortalization vector SSR #41. This retroviral vector contains the hygromycin and SV40 T-antigen expression cassette flanked with FRT sites and can be removed by the Flippase (FLP) recombinase. (**B**) Establishment of imPOD. The tsPC cells were infected with the packaged SSR #41 retrovirus and selected in hygromycin-containing medium for 5 days, yielding imPOD cells, which grow rapidly in conventional complete DMEM at 37 °C and can be passaged extensively (***a***). As positive and negative controls, the parental tsPC cells were grown under nonpermissive conditions (at 37 °C, no γ-interferon) (***b***) or under permissive conditions (at 33 °C with 100U/ml γ-interferon) (***c***). Representative results are shown. (**C**) Expression of SV40 T-antigen in imPOD and tsPC cells. Both imPOD and tsPC cells were cultured at the indicated conditions for 24 h. Total RNA was isolated and subjected to reverse transcription and TqPCR analysis of SV40 T antigen expression. Gapdh served as a reference gene. "*" $p < 0.05$ and "**" $p < 0.01$ when compared with the tsPC-37 °C group.

Tubulin and Vinculin) were expressed in the imPOD cells. Nephrin is a transmembrane protein located at podocyte slit diaphragm.[6] We found that Nephrin expression was readily detected by immunofluorescence (Fig. 3B). The cell body and primary processes of podocytes contain all three types of cytoskeletal elements (e.g., mictotubules, intermediate filaments and microfilaments) and podocyte microtubules are essential for the formation and maintenance of podocyte primary processes. We detected a high level of Tubulin expression in both imPOD cells and tsPC-33 °C cells as previously reported (Fig. 3B).[7] Furthermore, cell—matrix interactions and podocyte intercellular junctions are essential for maintaining the glomerular filtration barrier. Vinculin is a cytoplasmic protein and able to couple actin filaments to integrin-mediated cell—matrix adhesions and to cadherin-based intercellular junctions.[65] We detected the expression of Vinculin at focal contacts by immunofluorescence (Fig. 3B). Interestingly, the distribution of Vinculin revealed the arrangement of focal contacts in tsPC-33 °C and imPOD cells was a random pattern rather than predominant localization at the tips of processes in arborized cells as reported.[7] Taken together, our results demonstrate that the imPOD cells express most of the podocyte-specific markers, similar to that of the parental tsPC cells.

FLP recombinase-mediated removal of SV40 T antigen diminishes the proliferative activity of the imPOD cells

As shown in Fig. 1A, the immortalizing gene SV40 T antigen can be excised by the expression of FLP recombinase. We tested whether the SV40 T antigen-mediated immortalization could be effectively reversed in the imPOD cells. We

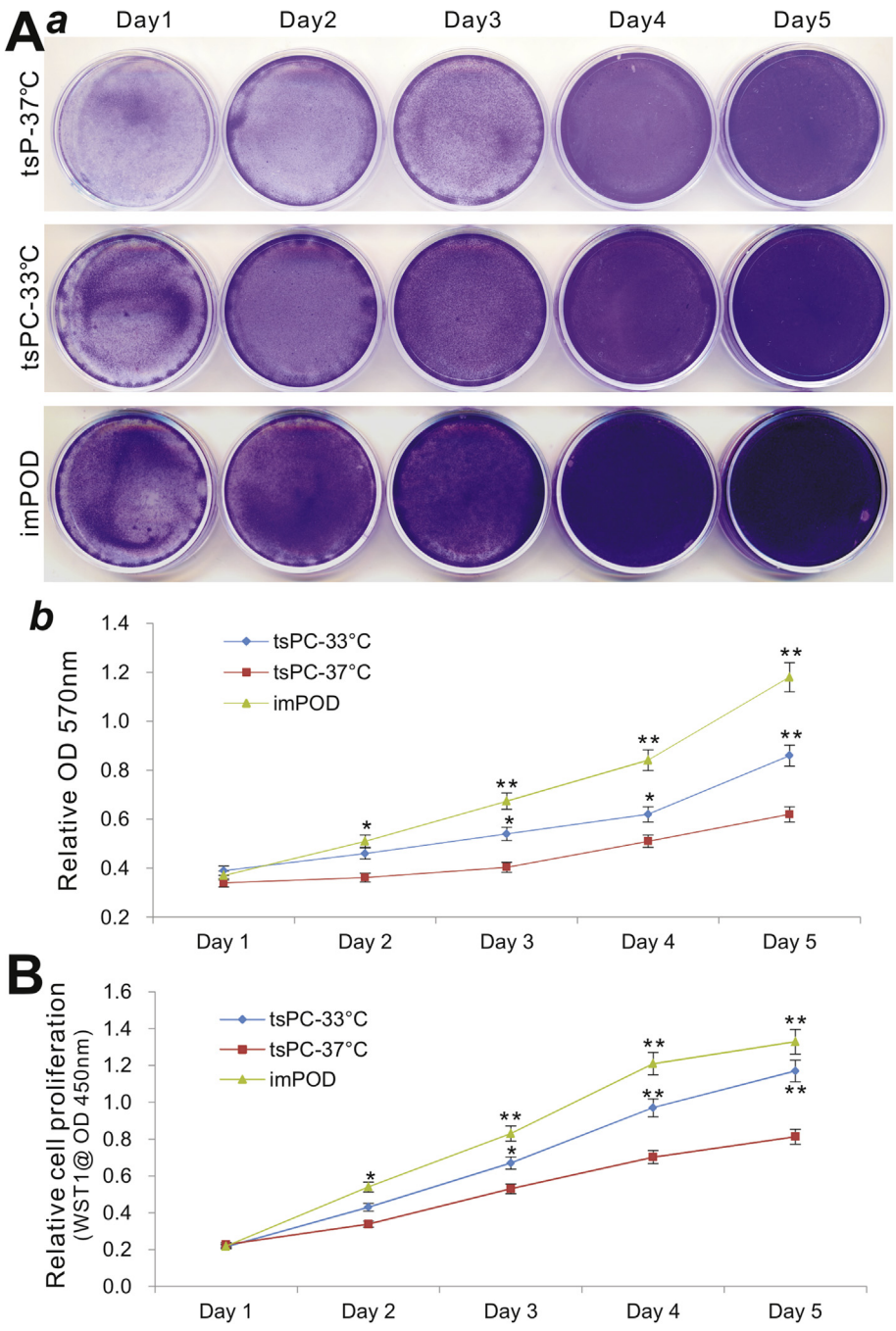

Figure 2 The imPOD cells exhibit high proliferative activity. (**A**) Cell proliferation assay assessed by crystal violet staining. Same numbers of parental tsPC (at 33 °C + 100U/ml γ-interferon, or 37 °C without γ-interferon) and imPOD cells were seeded at a low density and fixed for crystal violet staining at the indicated time points (***a***). The stained cells were dissolved for quantitative determination at A570 nm (***b***). The assays were performed in three independent batches of experiments. "*" $p < 0.05$ and "**" $p < 0.01$ when compared with the tsPC-37 °C group. (**B**) Cell proliferation assessed by WST-1 assay. Same numbers of parental tsPC (at 33 °C + 100U/ml γ-interferon, or 37 °C without γ-interferon) and imPOD cells were seeded at a low density. At the indicated time points, WST-1 substrate was added to the cell culture medium and assessed for A450 nm readings. Assays were performed in triplicate. "*" $p < 0.05$ and "**" $p < 0.01$ when compared with the tsPC-37 °C group.

previously constructed a recombinant adenoviral vector Ad-FLP as an effective tool to deliver FLP into mammalian cells/tissues.[18,52] We showed that the imPOD cells were infected by Ad-FLP or Ad-GFP with a high efficiency, and that the infected imPOD cells grew at a much slower rate (Fig. 4A, panel *a*). Furthermore, we sought to quantitatively determine the efficiency of FLP-mediated removal of the SV40 T antigen, which is complicated by the presence of ts-mutant form of SV40 T antigen in the imPOD cells. Instead, we analyzed the effect of FLP treatment on hygromycin expression in the imPOD cells. As expected, the efficient removal of hygromycin by FLP was confirmed by qPCR

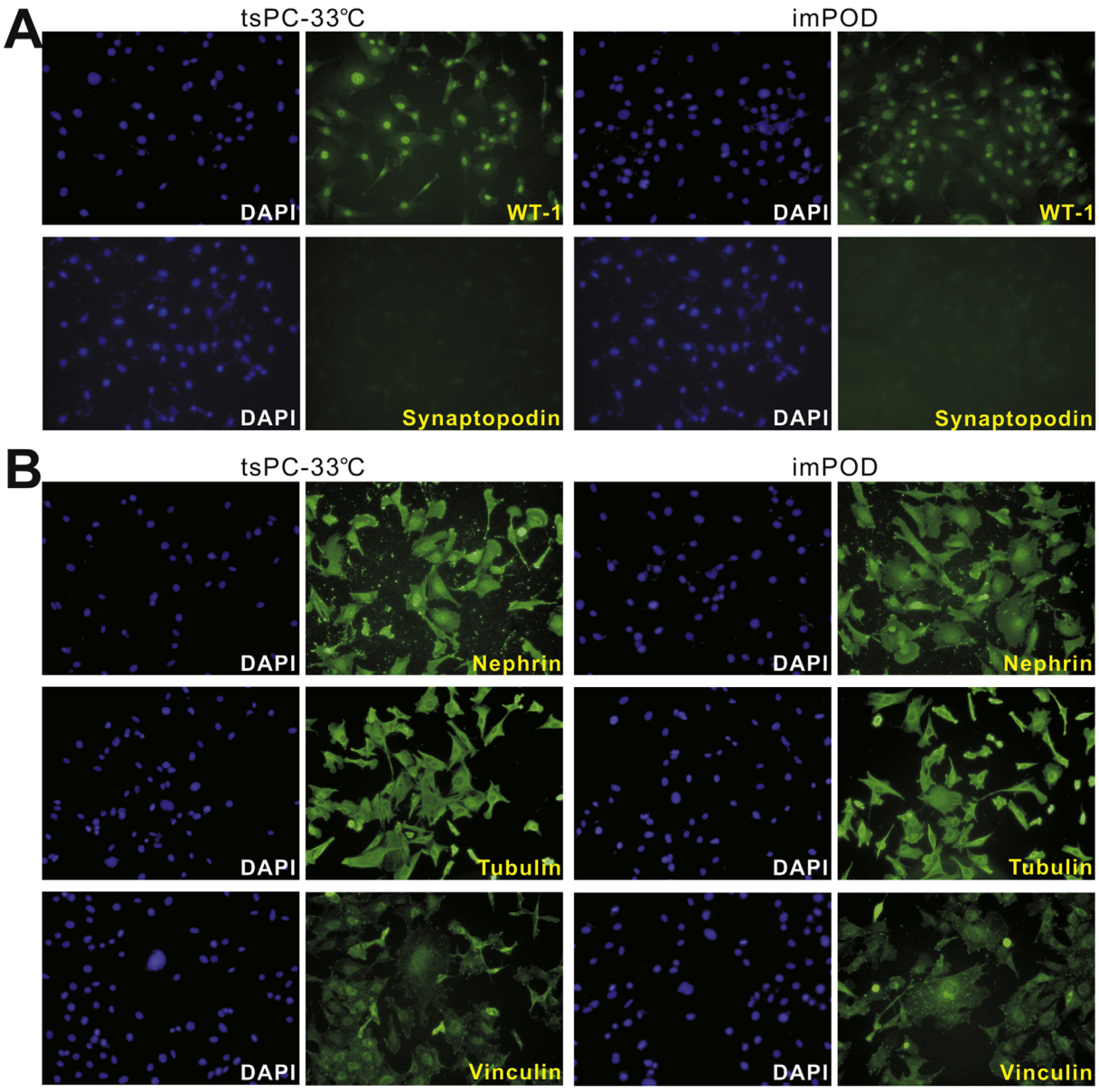

Figure 3 The imPOD cells express podocyte markers. The imPOD and parental tsPC (at 33 °C + 100U/ml γ-interferon) cells were seeded at subconfluence and stained with antibodies against the podocyte specific marker (WT-1) and Synaptopodin (**A**), as well as the slit diaphragm complex related markers (Nephrin, Tubulin and Vinculin) (**B**). Stains without primary antibodies were used as negative controls. Cell nuclei were counter-stained with DAPI. Representative images are shown.

analysis in the Ad-FLP infected imPOD cells, compared with that in the Ad-GFP control group (Fig. 4A, panel *b*).

In fact, we demonstrated that the cell proliferation rates of the Ad-FLP-infected imPOD cells were inversely correlated with the adenovirus titers of the Ad-FLP, but not Ad-GFP mock control, as assessed by crystal violet staining (Fig. 4B, panel *a*). Quantitative analysis of the crystal violet stains confirmed a trend of the decreased cell growth associated with the increased Ad-FLP titers (as expressed in MOIs, or multiplicities of infection) (Fig. 4B, panel *b*). Collectively, these results strongly indicate that the immortalization phenotype of the imPOD cells should be effectively reversed by FLP recombinase.

The imPOD cells are not tumorigenic in athymic nude mice

SV40 T antigen can stimulate cell proliferation and may increase the risk of tumorigenesis *in vivo*.[66] We sought to test if the established imPOD cells may possess tumor forming potential *in vivo*. In order to effectively track the *in vivo* tumor growth with high sensitivity, we first established Caki-FLuc and imPOD-FLuc cell lines by stably expressing the firefly luciferase using our recently optimized piggyBac transposon system.[52,59] Caki-1 is a commonly-used human kidney carcinoma cell line and was used as a positive control. When both Caki-FLuc and imPOD-FLuc cell lines were

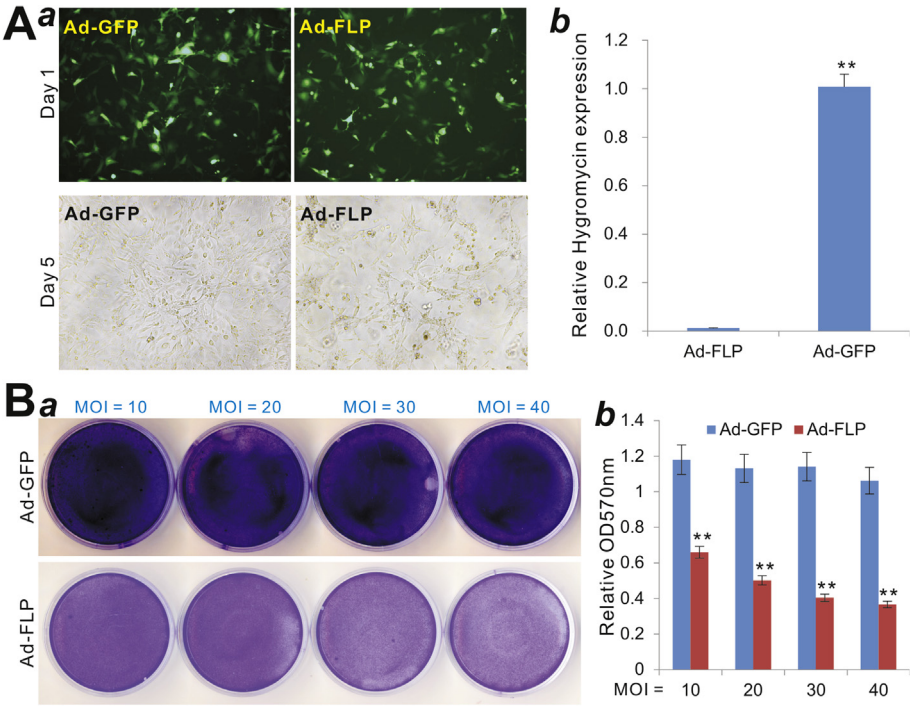

Figure 4 FLP recombinase-mediated removal of SV40 T-antigen effectively reverses the proliferative activity of imPOD cells. (**A**) Efficient removal of hygromycin from imPOD by Ad-FLP. Subconfluent imPOD cells were infected with Ad-GFP or Ad-FLP (***a***). At day 5, the imPOD cells infected with Ad-FLP exhibited much slower proliferation, compared with that infected with Ad-GFP (***a***). Representative images are shown. In addition, total RNA was isolated from the imPOD cells infected with Ad-FLP or Ad-GFP at day 3, and subjected to TqPCR analysis of the hygromycin expression (***b***). *Gapdh* served as a reference gene. All assay conditions were done in triplicate. "**" $p < 0.01$ compared with that of the Ad-FLP group. (**B**) Cell proliferation assay assessed by crystal violet staining. Subconfluent imPOD cells were infected with the indicated titers (MOI, multiplicity of infection) of Ad-FLP or Ad-GFP. At day 3, the infected cells were fixed and stained with crystal violet (***a***). The stained cells were dissolved and quantitatively measured at A570 nm (***b***). Each assay condition was performed in triplicate. Representative results are shown. "**" $p < 0.01$ compared with that of the Ad-GFP group.

subcutaneously injected into the athymic nude mice. The animals were subjected to whole body live bioluminescence imaging using Xenogen IVIS 200 at one day, one and two weeks after cell implantation. While similar bioluminescence signals ware readily detected in all injected animals in both groups at one day after injection, the signals decreased rather rapidly in the imPOD cell-injected mice at the one-week time point, and almost completely disappeared at the two-week time point (Fig. 5A), which was further confirmed by a quantitative analysis (Fig. 5B). Furthermore, we monitored the animals for up to four weeks and did not observe any tumor-like masses in the imPOD-FLuc injection group, while the Caki-FLuc injection group formed readily detectable tumor masses (data not shown). Collectively, these results strongly suggest that the imPOD cells may be not tumorigenic *in vivo* even though they possess long-term proliferative activity.

TGF-β1 induces podocyte injury-like response in the imPOD cells

Podocyte injury and dysfunction is implicated in proteinuria associated with chronic kidney disease and renal fibrosis.[4,67] Podocytes are responsible for the maintenance of the glomerular basement membrane, whose functions are compromised in the diabetic glomerulus.[68] TGF-β1 is considered as a key initiator of podocyte injuries.[69,70] We tested whether the imPOD cells were responsive to TGF-β1 stimulation and exhibited podocytopathy phenotypes. To accomplish this, we co-infected the imPOD cells with Ad-TGF-β1 and Ad-FLP or Ad-RFP. As a positive control, the parental tsPC cells (cultured under nonpermissive condition, tsPC-37 °C) were infected with Ad-TGF-β1 or Ad-RFP. At 72 h after infection, total RNA was isolated from the infected cells and subjected to qPCR analysis. The qPCR analysis confirmed a high level of adenovirus-mediated TGFβ1 expression in both imPOD and tsPC-37 °C cells (Fig. 6). Furthermore, TGFβ1 was shown to suppress the expression of the slit diaphragm-associated proteins P-Cadherin and zonula occludens-1 (ZO-1) in both groups (Fig. 6). We also demonstrated that exogenous TGFβ1 effectively induced the expression of mesenchymal markers, α-SMA, Vimentin and Nestin in the imPOD cells and the tsPC cells (Fig. 6). As a major autocrine growth factor induced by TGF-β1, CTGF mRNA expression was significantly up-regulated by TGFβ1 in both groups (Fig. 6). Lastly, TGFβ1 is involved in glomerular basement membrane (GBM) thickening and mesangial matrix expansion, and type I collagen is one of

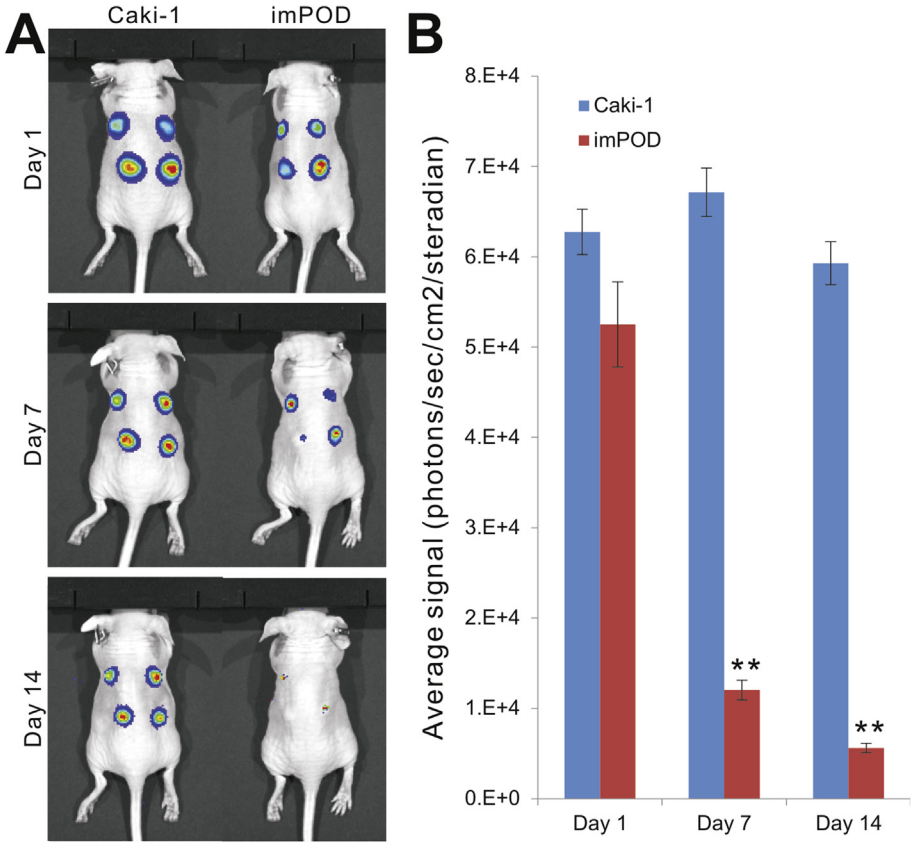

Figure 5 **The imPOD cells are not tumorigenic *in vivo*.** The human renal cancer line Caki-1 and imPOD cells were stably labeled with firefly luciferase, and injected subcutaneously into athymic nude mice (10^6 cells per injection, n = 5 mice/group). The animals were subjected to Xenogen IVIS 200 imaging at the indicated time points (**A**). Unlike that in the Caki-1 group, no masses were observed in the imPOD group for up to 4 weeks post injection. Representative results are shown. The average bioluminescence signals were quantitatively analyzed by using the Living Image software (**B**). "**" $p < 0.01$ compared with that of the Caki-1 injection group.

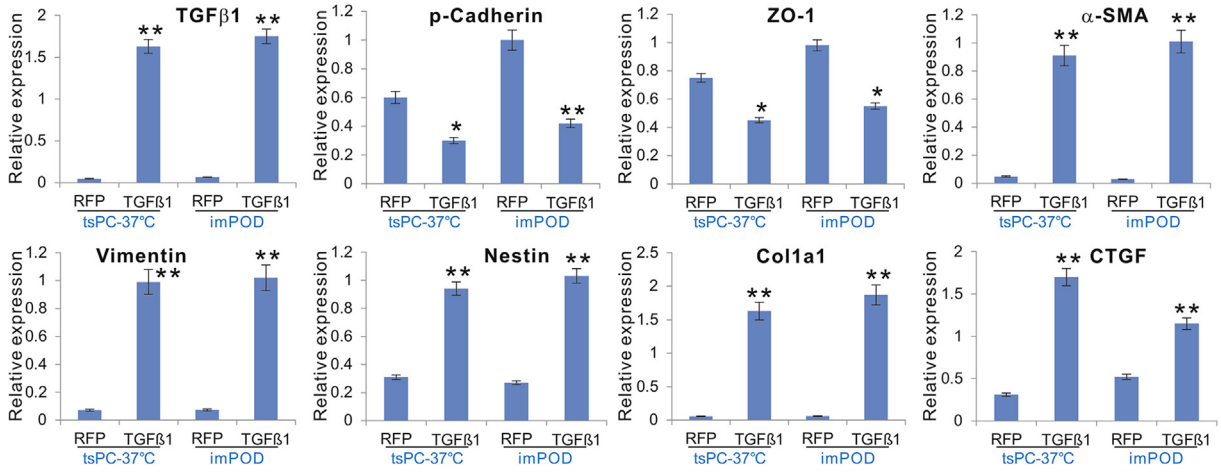

Figure 6 **TGFβ1 induces renal fibrosis-related markers in imPOD cells.** Subconfluent imPOD were co-infected with Ad-TGFβ1 and Ad-FLP or Ad-RFP, while the parental tsPC cells cultured under nonpermissive condition (tsPC-37 °C) were infected with Ad-RFP or Ad-TGFβ1. Total RNA was isolated at 72 h post infection and subjected to TqPCR analysis of a panel of mouse genes of interest including TGFβ1, P-cadherin, zonula occludens-1 (ZO-1), α-SMA, Vimentin, Nestin, CTGF and Collagen I (Col1a1). All assays were done in triplicate, and Gapdh served as a reference gene. "*" $p < 0.05$ and "**" $p < 0.01$ when compared with the respective Ad-RFP infection groups.

the matrix components.[70] Accordingly, we found that TGFβ1 effectively up-regulated the expression of Col1a1 in the imPOD cells, as well as in the parental tsPC cells (Fig. 6). Taken together, our results demonstrate that the imPOD cells may function as normal podocytes upon the removal of the SV40 T-antigen immortalization gene.

Discussion

The glomerular podocytes play an important role in the physiology and pathophysiology of the glomerulus. Podocytes are involved in a variety of glomerular functions, including GBM-turnover, maintenance of filtration barrier, support of the capillary tuft, regulation of glomerular filtration and immunological functions.[1,2] The functional or structural alterations in the podocytes may cause glomerular dysfunction and degeneration. Nonetheless, it is rather difficult to study podocyte functions *in vitro* as mature podocytes lose their proliferative capacity in the full differentiated state.[1,6] Thus, the establishment of conditionally immortalized podocytes made by Mundel et al was a major step toward a better understanding of this unique type of cells.[7] In this system, the conditionally immortalized podocyte cells (tsPC) were established using a special culture system in combination with H-2Kb-tsA58 transgenic mice.[7] Culturing podocyte cells at 33 °C with γ-interferon (permissive conditions) induces cell proliferation and maintains an epithelial phenotype. On the other hand, podocytes cultured at 37 °C without γ-interferon (non-permissive conditions) lose the activity of SV40 large T antigen and then enter a state of growth arrest and differentiation.[7] However, it takes approximately 14 days for the tsPC cells to completely lose activity of SV40 T antigen.

Here we seek to simplify the podocyte culture system and establish a reversibly immortalized podocyte line using the FRT-flanked SV40 T-antigen immortalization system. Using the reversible SV40 T antigen-based immortalization system, we have successfully immortalized primary numerous cell lines, including embryonic fibroblasts, adipose-derived MSCs (iMADs), stem cells from dental apical papilla, hepatic progenitor cells, mouse melanocytes, calvarial mesenchymal progenitor cells, articular chondrocytes, fetal heart progenitors, bone marrow stromal stem cells, and human cranial suture progenitors.[9–21] In this study, we utilized the FRT-flanked SV40 T antigen and successfully established the mouse podocyte imPOD line.

We demonstrate that the imPOD cells express most of the podocyte markers. It has been reported that the expression of Wilms' tumor 1(WT-1) can be detected in the visceral epithelial cells (podocytes) of the mature glomerulus throughout life.[71] It was also reported that WT-1 protein may be involved in maintaining podocyte lineage and differentiation potential.[2,7] The imPOD cells expressed WT-1 protein just as the conditionally immortalized mouse podocyte cell lines (tsPC-33 °C). Interestingly, Synaptopodin is a differentiation–specific marker and is not detected in both imPOD and tsPC-33 °C cells. In addition, the expression of Nephrin, a newly identified transmembrane protein located at podocyte slit diaphragm,[7] was expressed in the imPODs cells. The imPOD cells, like tsPC-33 °C cells, also express Vinculin, a cytoplasmic protein important for maintaining the glomerular filtration barrier. Nonetheless, the imPOD cells do not possess *in vivo* tumorigenicity.

Furthermore, the imPOD cells are responsive to the fibrogenic cytokine TGFβ1 stimulation and exhibit podocyte injury-like phenotypes. Podocyte injury is one of the major stimuli resulting in an impaired glomerular filtration, which is manifested by proteinuria in the clinical setting.[4] As a potent fibrogenic cytokine TGFβ1 is upregulated in virtually all kinds of chronic kidney diseases[72,73] and is a well-characterized pathogenic factor that dysregulates podocyte structure and functions.[72–74] TGFβ1 was shown to induce podocytes to undergo epithelial–mesenchymal transition (EMT),[75] acquiring some mesenchymal phenotype while losing some markers of glomerular epithelial cell differentiation.[76] Consistent with the pathophysiology of podocytes, the expression of glomerular epithelial markers (Nephrin, P-Cadherin, and ZO-1) was decreased in the imPOD cells upon TGFβ1 stimulation, whereas the expression of mesenchymal markers (αSMA, Vimentin, and Nestin) and matrix components (fibronectin, type I collagen) was upregulated by TGFβ1. Taken together, the engineered imPOD cells should provide a valuable *in vitro* cell model to study podocyte biology.

Immortalization of primary mammalian cells is usually accomplished by overexpressing oncogenes, such as telomerase (TERT), KRAS, c-MYC, CDK4, and/or inactivating tumor suppressor genes, such as p53, Rb and $p16^{INK}$ [11,66]. It is well established that the ability of SV40 T antigen to immortalize cells is mediated by its ability to form a complex with p53 and hence inhibit p53 functions. However, the exact molecular mechanisms underlying SV40 T antigen-induced immortalization remain to be fully understood.[11] Nonetheless, unlike the above-mentioned oncogenes, SV40 T antigen-transformed cells are usually not tumorigenic,[77,78] which has been further confirmed in our *in vivo* studies with the imPOD cells.

In summary, we demonstrate that mouse podocytes can be reversibly immortalized with a FRT-flanked SV40 T-antigen expression system. The reversibly immortalized imPOD cells exhibit long-term high proliferative activity, which can be effectively reversed by FLP recombinase. The imPOD cells express most of the podocyte markers, do not form tumors *in vivo* and exhibit the characteristics similar to mature podocytes upon TGFβ1 stimulation. Thus, the imPOD should be a valuable resource to study podocyte biology both under normal and under pathological conditions.

Conflict of interest

The authors declare no conflicts of interest.

Acknowledgments

The authors wish to thank Dr. Philippe Leboulch of Harvard Medical School for the generous provision of the SSR #41 vector, and Dr. Yun-Chun Li of The University of Chicago for the kind provision of the SV40 T-antigen ts-mutant-immortalized mouse podocytes. The reported work was supported in part by research grants from the National

Institutes of Health (CA226303 to TCH) and the National Key Research and Development Program of China (2016YFC1000803 and 2011CB707906 to TCH). This project was also supported in part by The University of Chicago Cancer Center Support Grant (P30CA014599) and the National Center for Advancing Translational Sciences of the National Institutes of Health through Grant Number UL1 TR000430. Funding sources were not involved in the study design; in the collection, analysis and interpretation of data; in the writing of the report; and in the decision to submit the paper for publication.

Appendix A. Supplementary data

Supplementary data related to this article can be found at https://doi.org/10.1016/j.gendis.2018.04.003.

References

1. Pavenstadt H, Kriz W, Kretzler M. Cell biology of the glomerular podocyte. *Physiol Rev*. 2003;83(1):253—307.
2. Mundel P, Kriz W. Structure and function of podocytes: an update. *Anat Embryol (Berl)*. 1995;192(5):385—397.
3. Romagnani P, Remuzzi G, Glassock R, et al. Chronic kidney disease. *Nat Rev Dis Primers*. 2017;3:17088.
4. Patrakka J, Tryggvason K. New insights into the role of podocytes in proteinuria. *Nat Rev Nephrol*. 2009;5(8):463—468.
5. Levey AS, Coresh J. Chronic kidney disease. *Lancet*. 2012; 379(9811):165—180.
6. Saleem MA, O'Hare MJ, Reiser J, et al. A conditionally immortalized human podocyte cell line demonstrating nephrin and podocin expression. *J Am Soc Nephrol*. 2002;13(3): 630—638.
7. Mundel P, Reiser J, Zuniga Mejia Borja A, et al. Rearrangements of the cytoskeleton and cell contacts induce process formation during differentiation of conditionally immortalized mouse podocyte cell lines. *Exp Cell Res*. 1997;236(1):248—258.
8. Westerman KA, Leboulch P. Reversible immortalization of mammalian cells mediated by retroviral transfer and site-specific recombination. *Proc Natl Acad Sci U S A*. 1996; 93(17):8971—8976.
9. Bi Y, He Y, Huang J, et al. Functional characteristics of reversibly immortalized hepatic progenitor cells derived from mouse embryonic liver. *Cell Physiol Biochem*. 2014;34(4): 1318—1338.
10. Bi Y, He Y, Huang JY, et al. Induced maturation of hepatic progenitor cells in vitro. *Braz J Med Biol Res*. 2013;46(7): 559—566.
11. Huang E, Bi Y, Jiang W, et al. Conditionally immortalized mouse embryonic fibroblasts retain proliferative activity without compromising multipotent differentiation potential. *PLoS One*. 2012;7(2):e32428.
12. Li M, Chen Y, Bi Y, et al. Establishment and characterization of the reversibly immortalized mouse fetal heart progenitors. *Int J Med Sci*. 2013;10(8):1035—1046.
13. Huang J, Bi Y, Zhu GH, et al. Retinoic acid signalling induces the differentiation of mouse fetal liver-derived hepatic progenitor cells. *Liver Int*. 2009;29(10):1569—1581.
14. Yang K, Chen J, Jiang W, et al. Conditional immortalization establishes a repertoire of mouse melanocyte progenitors with distinct melanogenic differentiation potential. *J Invest Dermatol*. 2012;132(10):2479—2483.
15. Lamplot JD, Liu B, Yin L, et al. Reversibly immortalized mouse articular chondrocytes acquire long-term proliferative capability while retaining chondrogenic phenotype. *Cell Transplant*. 2015;24(6):1053—1066.
16. Song D, Zhang F, Reid RR, et al. BMP9 induces osteogenesis and adipogenesis in the immortalized human cranial suture progenitors from the patent sutures of craniosynostosis patients. *J Cell Mol Med*. 2017;21(11):2782—2795.
17. Wang J, Zhang H, Zhang W, et al. Bone morphogenetic Protein-9 (BMP9) effectively induces osteo/odontoblastic differentiation of the reversibly immortalized stem cells of dental apical papilla. *Stem Cells Dev*. 2014;23(12):1405—1416.
18. Lu S, Wang J, Ye J, et al. Bone morphogenetic protein 9 (BMP9) induces effective bone formation from reversibly immortalized multipotent adipose-derived (iMAD) mesenchymal stem cells. *Am J Transl Res*. 2016;8(9):3710—3730.
19. Denduluri SK, Scott B, Lamplot JD, et al. Immortalized mouse achilles tenocytes demonstrate long-term proliferative capacity while retaining tenogenic properties. *Tissue Eng Part C Meth*. 2016;22(3):280—289.
20. Shenaq DS, Teven CM, Seitz IA, et al. Characterization of reversibly immortalized calvarial mesenchymal progenitor cells. *J Craniofac Surg*. 2015;26(4):1207—1213.
21. Hu X, Li L, Yu X, et al. CRISPR/Cas9-mediated reversibly immortalized mouse bone marrow stromal stem cells (BMSCs) retain multipotent features of mesenchymal stem cells (MSCs). *Oncotarget*. 2017;8(67):111847—111865.
22. Wu N, Zhang H, Deng F, et al. Overexpression of Ad5 precursor terminal protein accelerates recombinant adenovirus packaging and amplification in HEK-293 packaging cells. *Gene Ther*. 2014;21(7):629—637.
23. Wei Q, Fan J, Liao J, et al. Engineering the rapid adenovirus production and amplification (RAPA) cell line to expedite the generation of recombinant adenoviruses. *Cell Physiol Biochem*. 2017;41(6):2383—2398.
24. Bi Y, Huang J, He Y, et al. Wnt antagonist SFRP3 inhibits the differentiation of mouse hepatic progenitor cells. *J Cell Biochem*. 2009;108(1):295—303.
25. Su Y, Luo X, He BC, et al. Establishment and characterization of a new highly metastatic human osteosarcoma cell line. *Clin Exp Metastasis*. 2009;26(7):599—610.
26. Huang E, Zhu G, Jiang W, et al. Growth hormone synergizes with BMP9 in osteogenic differentiation by activating the JAK/STAT/IGF1 pathway in murine multilineage cells. *J Bone Miner Res*. 2012;27(7):1566—1575.
27. Wang Y, Deb DK, Zhang Z, et al. Vitamin D receptor signaling in podocytes protects against diabetic nephropathy. *J Am Soc Nephrol*. 2012;23(12):1977—1986.
28. He T-C. *Adenoviral Vectors. Adenoviral Vectors in Current Protocols in Human Genetics. Vol Unit 12.4*. New York: John Wiley & Sons, Inc; 2004:12.14.11—12.14.25.
29. He TC, Zhou S, da Costa LT, Yu J, Kinzler KW, Vogelstein B. A simplified system for generating recombinant adenoviruses. *Proc Natl Acad Sci U S A*. 1998;95(5):2509—2514.
30. Luo J, Deng ZL, Luo X, et al. A protocol for rapid generation of recombinant adenoviruses using the AdEasy system. *Nat Protoc*. 2007;2(5):1236—1247.
31. Breyer B, Jiang W, Cheng H, et al. Adenoviral vector-mediated gene transfer for human gene therapy. *Curr Gene Ther*. 2001; 1(2):149—162.
32. Lee CS, Bishop ES, Zhang R, et al. Adenovirus-mediated gene delivery: potential applications for gene and cell-based therapies in the new era of personalized medicine. *Genes Dis*. 2017;4(2):43—63.
33. Zhu GH, Huang J, Bi Y, et al. Activation of RXR and RAR signaling promotes myogenic differentiation of myoblastic C2C12 cells. *Differentiation*. 2009;78:195—204.
34. Hu N, Jiang D, Huang E, et al. BMP9-regulated angiogenic signaling plays an important role in the osteogenic

differentiation of mesenchymal progenitor cells. *J Cell Sci*. 2013;126(Pt 2):532—541.
35. Zhang H, Wang J, Deng F, et al. Canonical Wnt signaling acts synergistically on BMP9-induced osteo/odontoblastic differentiation of stem cells of dental apical papilla (SCAPs). *Biomaterials*. 2015;39:145—154.
36. Gao Y, Huang E, Zhang H, et al. Crosstalk between Wnt/beta-catenin and estrogen receptor signaling synergistically promotes osteogenic differentiation of mesenchymal progenitor cells. *PLoS One*. 2013;8(12):e82436.
37. Wang Y, Hong S, Li M, et al. Noggin resistance contributes to the potent osteogenic capability of BMP9 in mesenchymal stem cells. *J Orthop Res*. 2013;31(11):1796—1803.
38. Zhao C, Wu N, Deng F, et al. Adenovirus-mediated gene transfer in mesenchymal stem cells can be significantly enhanced by the cationic polymer polybrene. *PLoS One*. 2014;9(3):e92908.
39. Liao J, Wei Q, Fan J, et al. Characterization of retroviral infectivity and superinfection resistance during retrovirus-mediated transduction of mammalian cells. *Gene Ther*. 2017;24(6):333—341.
40. Fan J, Wei Q, Liao J, et al. Noncanonical Wnt signaling plays an important role in modulating canonical Wnt-regulated stemness, proliferation and terminal differentiation of hepatic progenitors. *Oncotarget*. 2017;8(16):27105—27119.
41. Zhang F, Li Y, Zhang H, et al. Anthelmintic mebendazole enhances cisplatin's effect on suppressing cell proliferation and promotes differentiation of head and neck squamous cell carcinoma (HNSCC). *Oncotarget*. 2017;8(8):12968—12982.
42. Deng Y, Wang Z, Zhang F, et al. A blockade of IGF signaling sensitizes human ovarian cancer cells to the anthelmintic niclosamide-induced anti-proliferative and anticancer activities. *Cell Physiol Biochem*. 2016;39(3):871—888.
43. Deng Y, Zhang J, Wang Z, et al. Antibiotic monensin synergizes with EGFR inhibitors and oxaliplatin to suppress the proliferation of human ovarian cancer cells. *Sci Rep*. 2015;5:17523.
44. Li Y, Wagner ER, Yan Z, et al. The calcium-binding protein S100A6 accelerates human osteosarcoma growth by promoting cell proliferation and inhibiting osteogenic differentiation. *Cell Physiol Biochem*. 2015;37(6):2375—2392.
45. He BC, Chen L, Zuo GW, et al. Synergistic antitumor effect of the activated PPARgamma and retinoid receptors on human osteosarcoma. *Clin Cancer Res*. 2010;16(8):2235—2245.
46. He BC, Gao JL, Zhang BQ, et al. Tetrandrine inhibits Wnt/beta-catenin signaling and suppresses tumor growth of human colorectal cancer. *Mol Pharmacol*. 2011;79(2):211—219.
47. Su Y, Wagner ER, Luo Q, et al. Insulin-like growth factor binding protein 5 suppresses tumor growth and metastasis of human osteosarcoma. *Oncogene*. 2011;30(37):3907—3917.
48. Luo Q, Kang Q, Si W, et al. Connective tissue growth factor (CTGF) is regulated by Wnt and bone morphogenetic proteins signaling in osteoblast differentiation of mesenchymal stem cells. *J Biol Chem*. 2004;279(53):55958—55968.
49. Luo X, Chen J, Song WX, et al. Osteogenic BMPs promote tumor growth of human osteosarcomas that harbor differentiation defects. *Lab Invest*. 2008;88(12):1264—1277.
50. Si W, Kang Q, Luu HH, et al. CCN1/Cyr61 is regulated by the canonical Wnt signal and plays an important role in Wnt3A-induced osteoblast differentiation of mesenchymal stem cells. *Mol Cell Biol*. 2006;26(8):2955—2964.
51. Wang N, Zhang H, Zhang BQ, et al. Adenovirus-mediated efficient gene transfer into cultured three-dimensional organoids. *PLoS One*. 2014;9(4):e93608.
52. Wang N, Zhang W, Cui J, et al. The piggyBac transposon-mediated expression of SV40 T antigen efficiently immortalizes mouse embryonic fibroblasts (MEFs). *PLoS One*. 2014;9(5):e97316.
53. Kong Y, Zhang H, Chen X, et al. Destabilization of heterologous proteins mediated by the GSK3beta phosphorylation domain of the beta-catenin protein. *Cell Physiol Biochem*. 2013;32(5):1187—1199.
54. Liao J, Wei Q, Zou Y, et al. Notch signaling augments BMP9-induced bone formation by promoting the osteogenesis-angiogenesis coupling process in mesenchymal stem cells (MSCs). *Cell Physiol Biochem*. 2017;41(5):1905—1923.
55. Liao J, Yu X, Hu X, et al. lncRNA H19 mediates BMP9-induced osteogenic differentiation of mesenchymal stem cells (MSCs) through Notch signaling. *Oncotarget*. 2017;8(32):53581—53601.
56. Zou Y, Qazvini NT, Zane K, et al. Gelatin-derived graphene-silicate hybrid materials are biocompatible and synergistically promote BMP9-induced osteogenic differentiation of mesenchymal stem cells. *ACS Appl Mater Interfaces*. 2017;9(19):15922—15932.
57. Untergasser A, Cutcutache I, Koressaar T, et al. Primer3—new capabilities and interfaces. *Nucleic Acids Res*. 2012;40(15):e115.
58. Zhang Q, Wang J, Deng F, et al. TqPCR: a touchdown qPCR assay with significantly improved detection sensitivity and amplification efficiency of SYBR Green qPCR. *PLoS One*. 2015;10(7). e0132666.
59. Chen X, Cui J, Yan Z, et al. Sustained high level transgene expression in mammalian cells mediated by the optimized piggyBac transposon system. *Genes Dis*. 2015;2(1):96—105.
60. Liao Z, Nan G, Yan Z, et al. The anthelmintic drug niclosamide inhibits the proliferative activity of human osteosarcoma cells by targeting multiple signal pathways. *Curr Cancer Drug Targets*. 2015;15(8):726—738.
61. Li R, Zhang W, Cui J, et al. Targeting BMP9-promoted human osteosarcoma growth by inactivation of notch signaling. *Curr Cancer Drug Targets*. 2014;14(3):274—285.
62. Pelletier J, Schalling M, Buckler AJ, Rogers A, Haber DA, Housman D. Expression of the Wilms' tumor gene WT1 in the murine urogenital system. *Genes Dev*. 1991;5(8):1345—1356.
63. Mundlos S, Pelletier J, Darveau A, Bachmann M, Winterpacht A, Zabel B. Nuclear localization of the protein encoded by the Wilms' tumor gene WT1 in embryonic and adult tissues. *Development*. 1993;119(4):1329—1341.
64. Mundel P, Heid HW, Mundel TM, Kruger M, Reiser J, Kriz W. Synaptopodin: an actin-associated protein in telencephalic dendrites and renal podocytes. *J Cell Biol*. 1997;139(1):193—204.
65. Lausecker F, Tian X, Inoue K, et al. Vinculin is required to maintain glomerular barrier integrity. *Kidney Int*. 2018;93(3):643—655.
66. vom Brocke J, Schmeiser HH, Reinbold M, Hollstein M. MEF immortalization to investigate the ins and outs of mutagenesis. *Carcinogenesis*. 2006;27(11):2141—2147.
67. Reiser J, Gupta V, Kistler AD. Toward the development of podocyte-specific drugs. *Kidney Int*. 2010;77(8):662—668.
68. Susztak K, Raff AC, Schiffer M, Bottinger EP. Glucose-induced reactive oxygen species cause apoptosis of podocytes and podocyte depletion at the onset of diabetic nephropathy. *Diabetes*. 2006;55(1):225—233.
69. Schiffer M, Bitzer M, Roberts IS, et al. Apoptosis in podocytes induced by TGF-beta and Smad7. *J Clin Invest*. 2001;108(6):807—816.
70. Lee HS, Song CY. Effects of TGF-beta on podocyte growth and disease progression in proliferative podocytopathies. *Kidney Blood Press Res*. 2010;33(1):24—29.
71. Guo JK, Menke AL, Gubler MC, et al. WT1 is a key regulator of podocyte function: reduced expression levels cause crescentic glomerulonephritis and mesangial sclerosis. *Hum Mol Genet*. 2002;11(6):651—659.

72. Schnaper HW, Jandeska S, Runyan CE, et al. TGF-beta signal transduction in chronic kidney disease. *Front Biosci (Landmark Ed)*. 2009;14:2448—2465.
73. Bottinger EP, Bitzer M. TGF-beta signaling in renal disease. *J Am Soc Nephrol*. 2002;13(10):2600—2610.
74. Wang D, Dai C, Li Y, Liu Y. Canonical Wnt/beta-catenin signaling mediates transforming growth factor-beta1-driven podocyte injury and proteinuria. *Kidney Int*. 2011;80(11): 1159—1169.
75. Li Y, Kang YS, Dai C, Kiss LP, Wen X, Liu Y. Epithelial-to-mesenchymal transition is a potential pathway leading to podocyte dysfunction and proteinuria. *Am J Pathol*. 2008; 172(2):299—308.
76. Herman-Edelstein M, Thomas MC, Thallas-Bonke V, Saleem M, Cooper ME, Kantharidis P. Dedifferentiation of immortalized human podocytes in response to transforming growth factor-beta: a model for diabetic podocytopathy. *Diabetes*. 2011; 60(6):1779—1788.
77. Nitta M, Katabuchi H, Ohtake H, Tashiro H, Yamaizumi M, Okamura H. Characterization and tumorigenicity of human ovarian surface epithelial cells immortalized by SV40 large T antigen. *Gynecol Oncol*. 2001;81(1):10—17.
78. Counter CM, Hahn WC, Wei W, et al. Dissociation among in vitro telomerase activity, telomere maintenance, and cellular immortalization. *Proc Natl Acad Sci U S A*. 1998;95(25): 14723—14728.